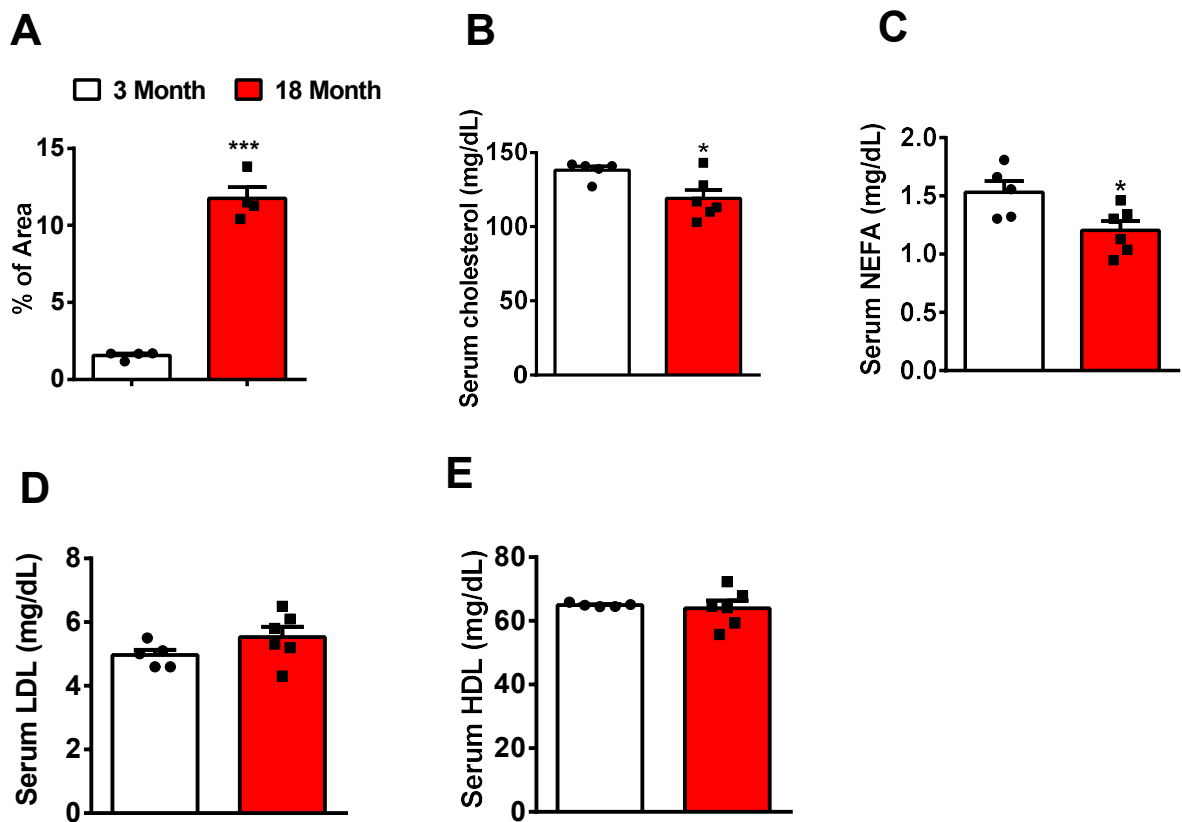


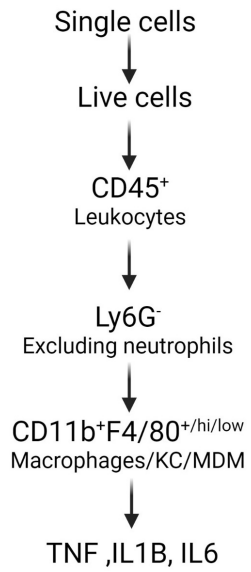
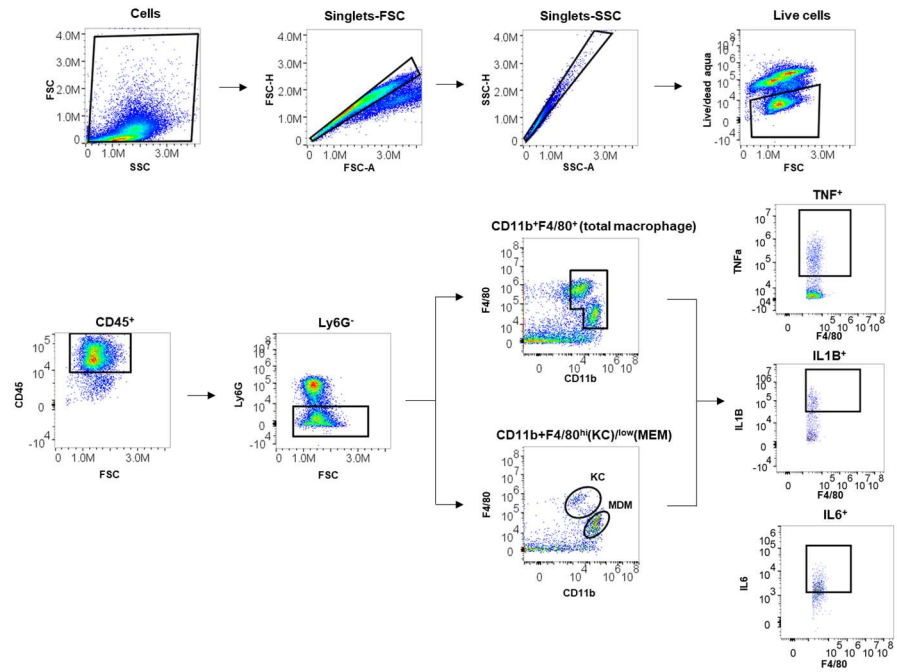
**Suppression of FOXO1 attenuates
inflamm-aging and improves liver
function during aging**

Supplementary Materials

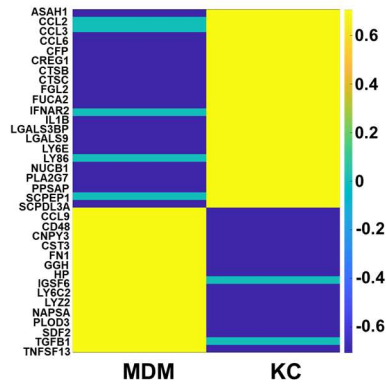
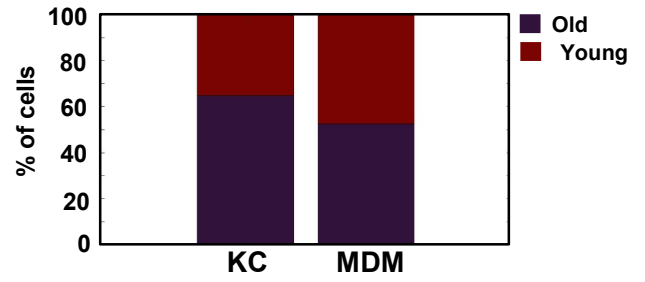
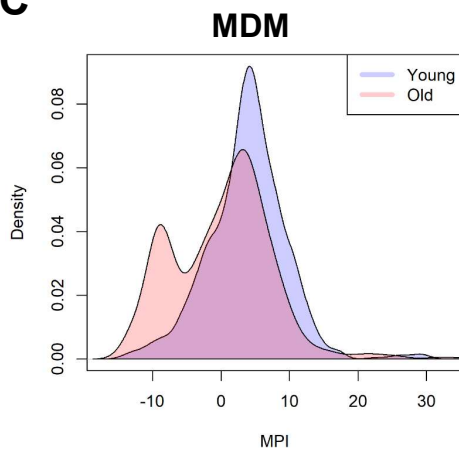
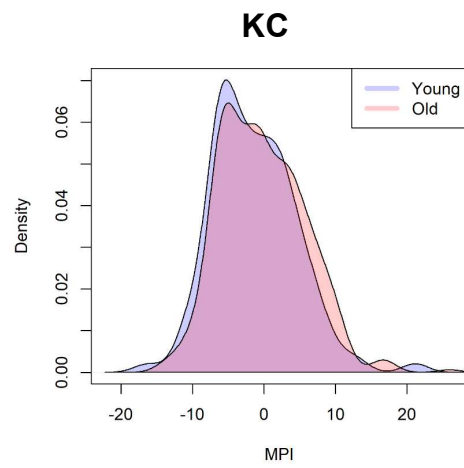
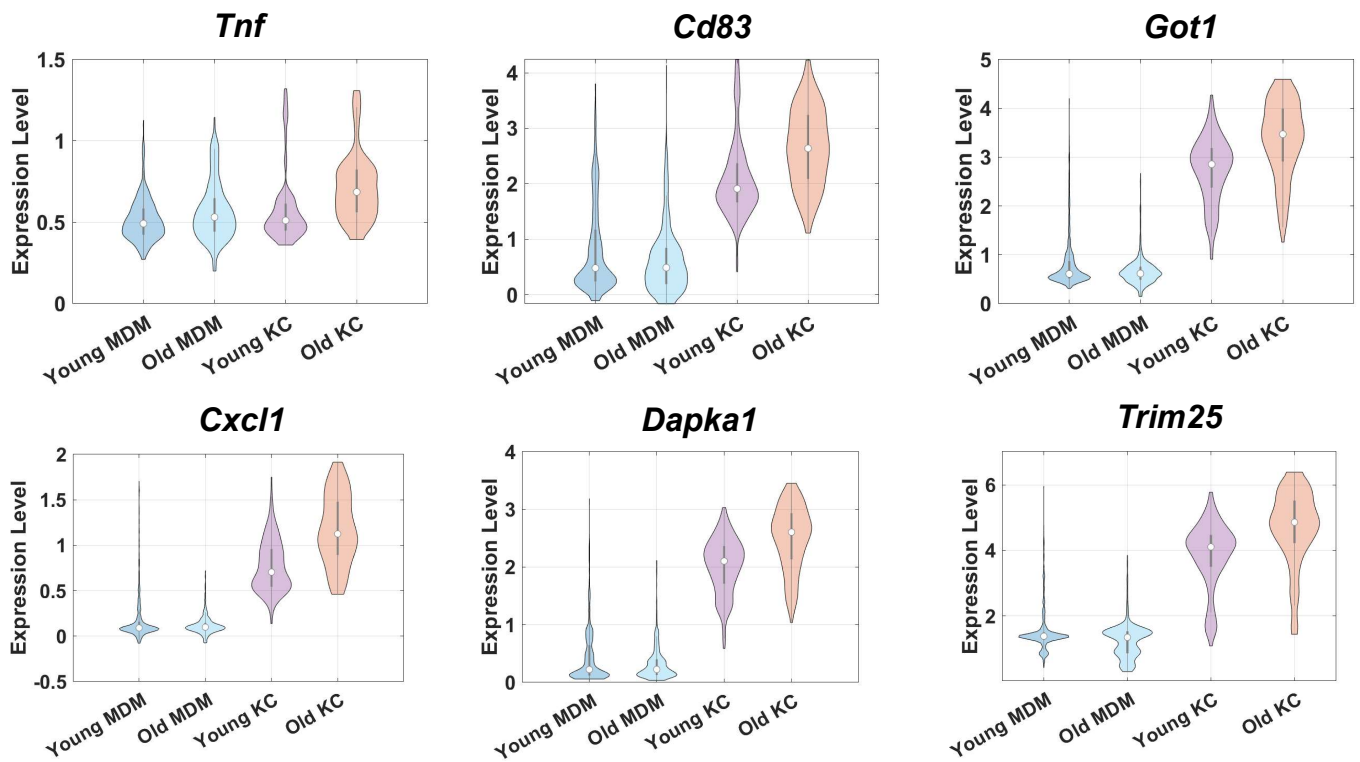


Supplementary Fig. 1 Lipid and glucose homeostasis are impaired in old mice

(A) Percentage of fat area in the livers of young and old mice, n=4 mice/group. (B-E) Serum cholesterol (B), NEFA (C), LDL (D), and HDL (E) in young and old mice, n=5-6 mice/group. All data are presented as mean \pm SEM. * p < 0.05.

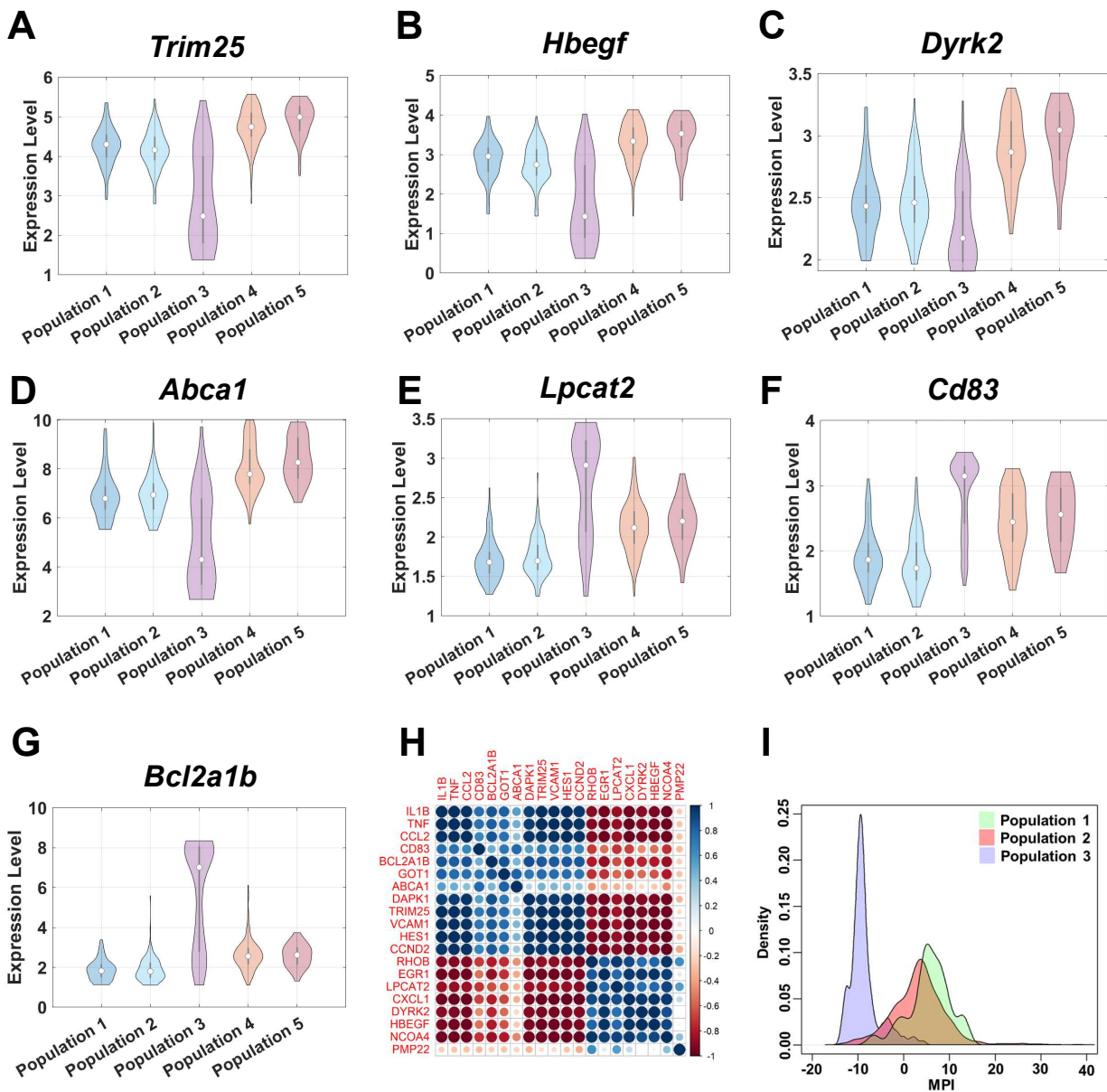
A**B**

Supplementary Fig. 2 . Flow cytometry gating strategy in control of NPC of liver. (A) Flow cytometry gating strategy of liver NPCs. (B) Representative scatter-blots of flow cytometry analysis.

A**B****C****D****E**

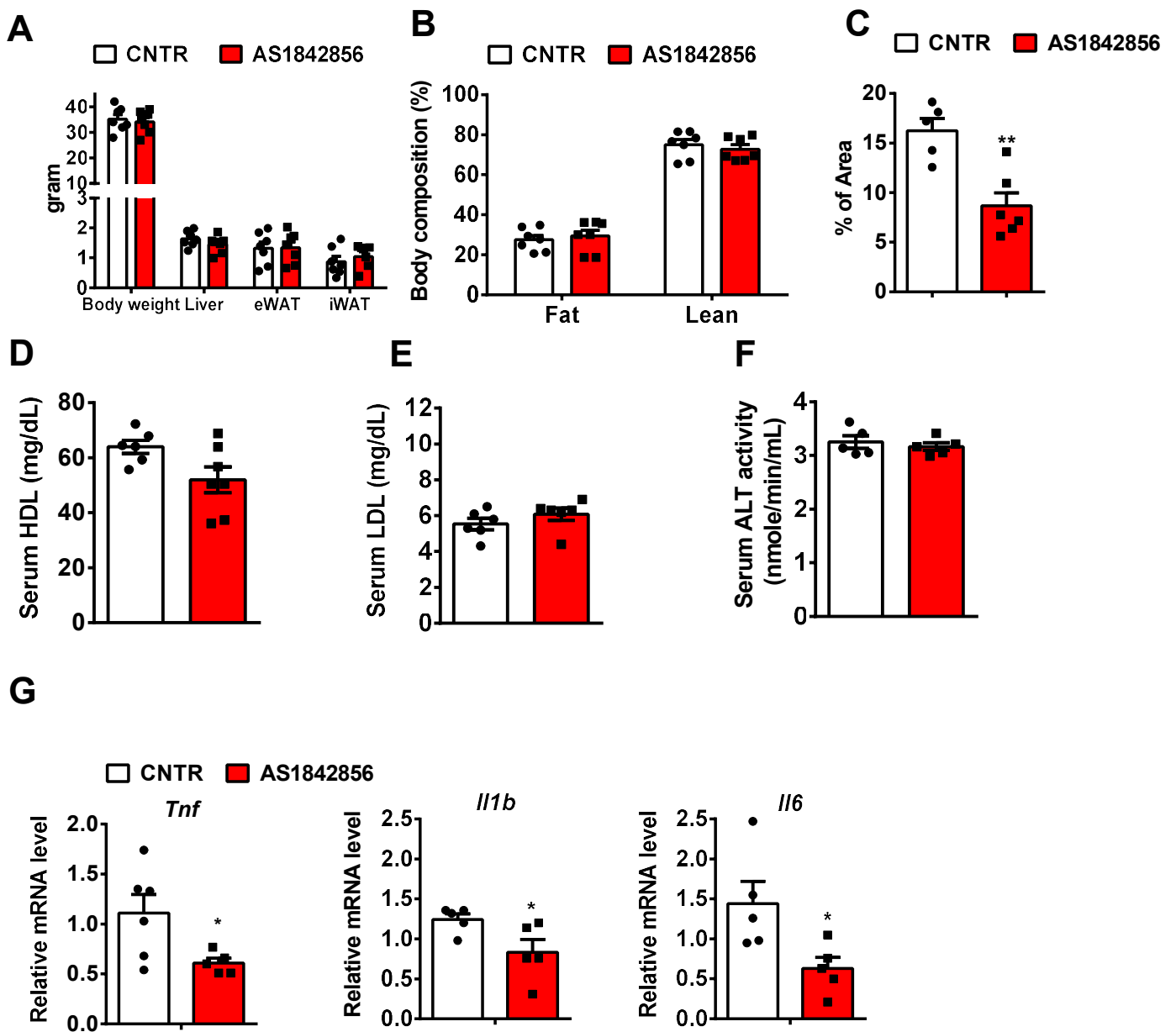
Supplementary Fig. 3 Kupffer cells contribute to the pro-inflammation in hepatic macrophages during aging.

(A) Heatmap of macrophage-secreted factor gene expression in KCs and MDMs. (B) Percent contribution of young and old mice in KCs and MDMs. (C) Macrophage polarization index (MPI) analysis in the KCs of young and old mice. (D) Macrophage polarization index (MPI) analysis in the MDMs of young and old mice. (E) Violin plots of ARKC genes in KCs and MDMs of young and old mice.



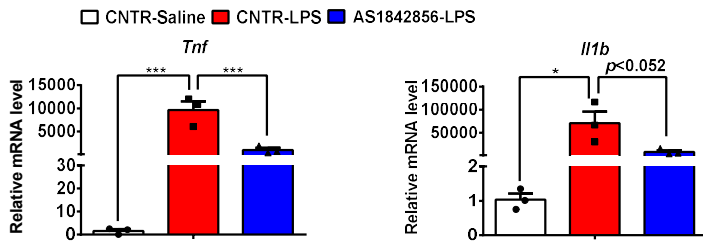
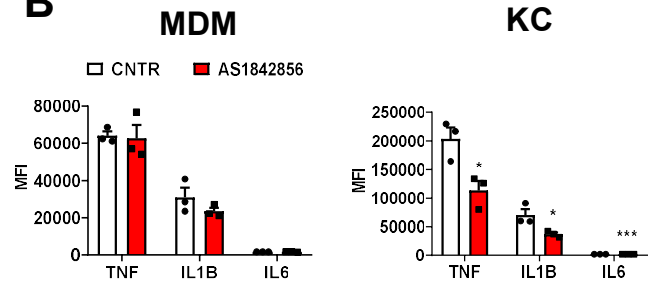
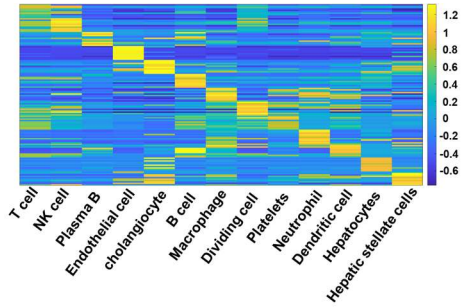
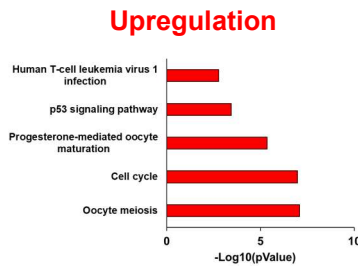
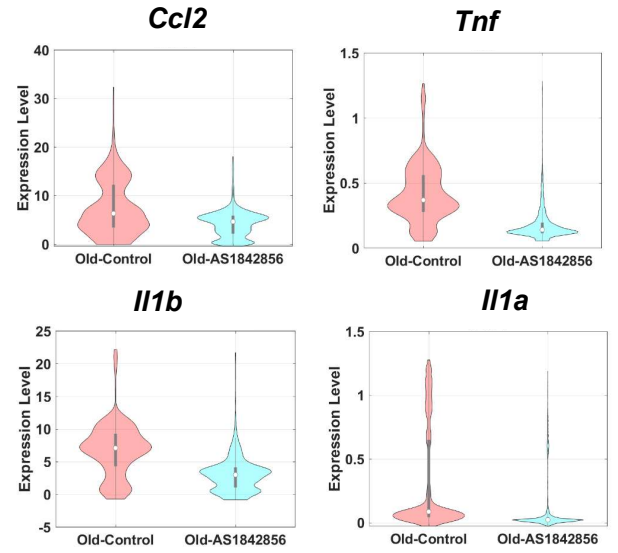
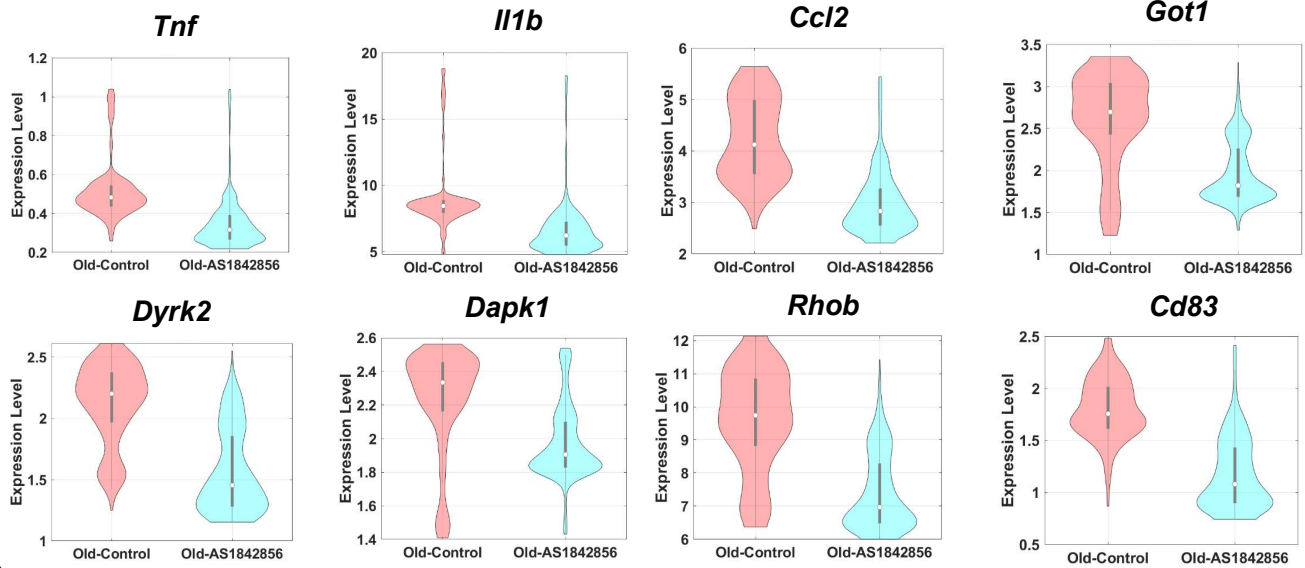
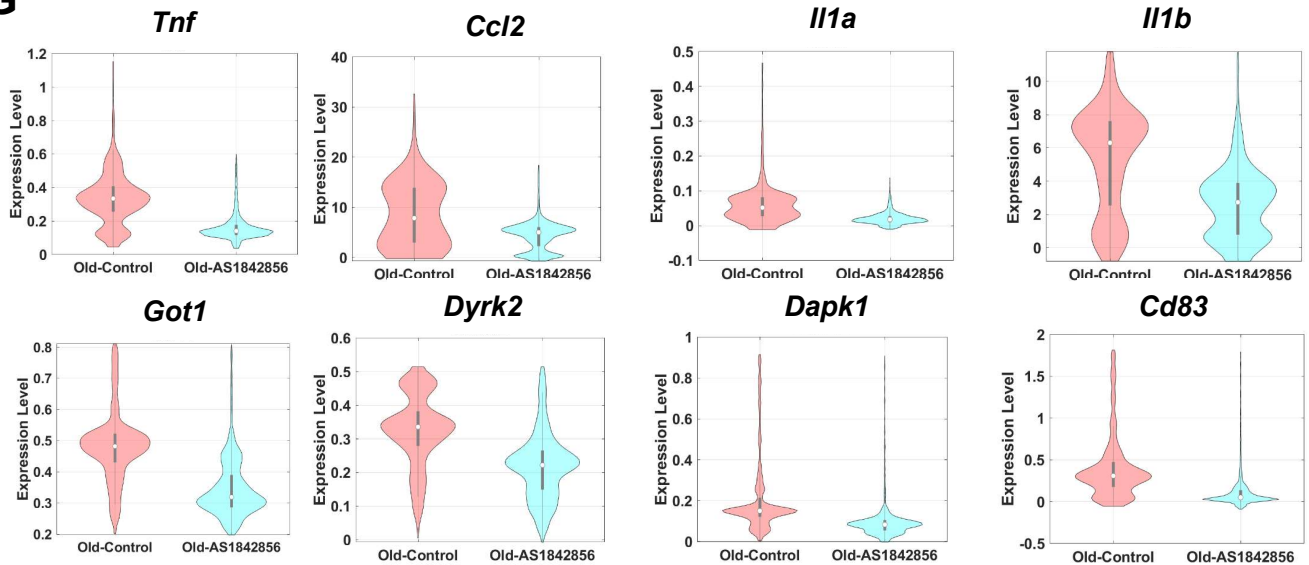
Supplementary Fig. 4 . KCs and MDMs are differentially affected during aging. inhibition improves aging-induced inflammation in macrophages.

(A-G) Violin plots of ARKC gene expression in KC populations. (H) Correlation between ARKC gene expression and pro-inflammatory cytokine gene expression in KC population 3. (I) Macrophage polarization index (MPI) analysis in MDM populations.

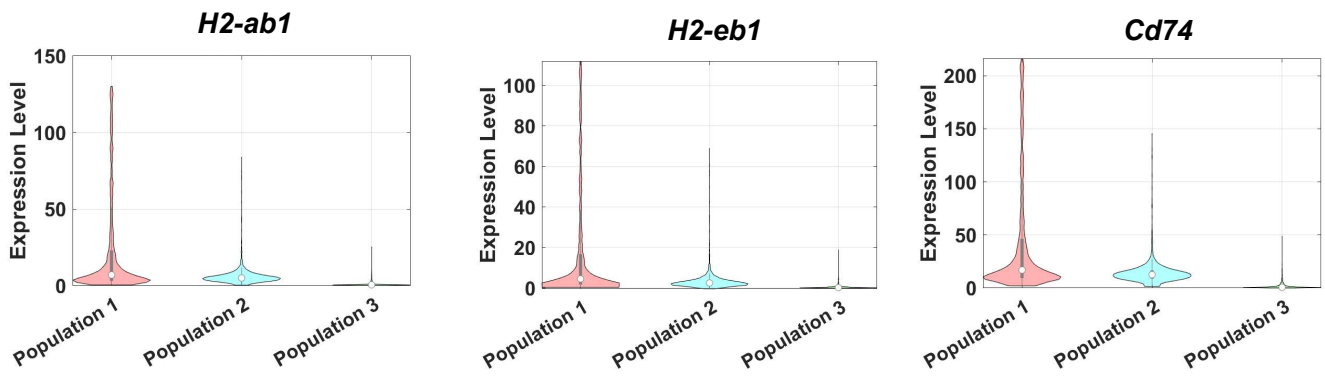
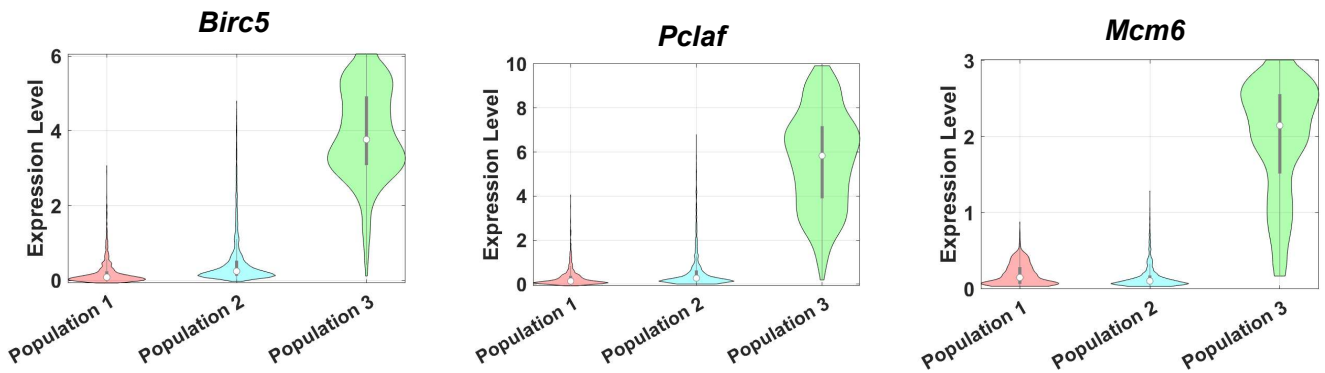


Supplementary Fig. 5 FOXO1 inhibition improves glucose homeostasis, hepatic steatosis, and chronic inflammation in old mice.

(A) Body weight and tissue weight in control and AS1842856-treated old mice, n=7. (B) Body composition in control and AS1842856-treated old mice, n=7. (C) Percentage of fat area in the livers of control and AS1842856-treated old mice, n=5-6 mice/group. (D-F) Serum HDL, LDL, and ALT in control and AS1842856-treated old mice, n=5-7. (G) The mRNA expression of pro-inflammatory cytokine genes in the PMs of control and AS1842856 treated old mice, n=5-6. All data are presented as mean \pm SEM. * $p < 0.05$, ** $p < 0.01$.

A**B****C****D****E****F****G**

Supplementary Fig. 6 FOXO1 inhibition improves pro-inflammation in hepatic macrophages during aging. (A) The mRNA expression of *Tnf* and *Il1b* in BMDMs treated with AS1842856, n=3. (B) The MFI of pro-inflammatory cytokines in the MDMs and KCs of control and AS1842856-treated old mice, n=3 mice/group. (C) Heatmap of cluster marker genes in the liver cells of control and AS1842856-treated old mice. (D) Pathway analysis of upregulated genes in the hepatic macrophages of AS1842856-treated old mice. (E) Violin plots of chemokine and pro-inflammatory cytokine genes in the hepatic macrophages of control and AS1842856-treated old mice. (F) Violin plots of pro-inflammatory cytokine and ARKC gene in the KCs of control and AS1842856-treated old mice. (G) Violin plots of pro-inflammatory cytokine and ARKC gene in the MDMs of control and AS1842856-treated old mice. All data are presented as mean \pm SEM. * p< 0.05, *** p< 0.001.

A**B**

Supplementary Fig. 7 FOXO1 inhibition rescues aging-induced phenotypes in KC but not in MDM.

(A) Violin plots of antigen presentation/process gene expression in MDM populations. (B) Violin plots of aging-induced MDM marker gene expression.